Effect of Gold Nanoparticles Size on Detection of Methylphosphonic Acid Hydrolysis Product of Nerve Agent

Pojol Fellyzra Elvya[1], Chieng Buong Woei[2], Ong Keat Khim[2,3*], Abd Rashid Jahwarhar Izuan[3], Osman Mohd Junaedy[3], Wan Yunus Wan Md Zin[4], Jamari Nor Laili-Azua[3] and Teoh Chin Chuang[5]

1. Department of Defence Science, Faculty of Defence Science and Technology, Universiti Pertahanan Nasional Malaysia, Kem Sungai Besi, 57000 Kuala Lumpur, MALAYSIA
2. Centre for Chemical Defence, Universiti Pertahanan Nasional Malaysia, Kem Sungai Besi, 57000 Kuala Lumpur, MALAYSIA
3. Department of Chemistry and Biology, Centre for Defence Foundation Studies, Universiti Pertahanan Nasional Malaysia, Kem Sungai Besi, 57000 Kuala Lumpur, MALAYSIA
4. Centre for Tropicalisation, Universiti Pertahanan Nasional Malaysia, Kem Sungai Besi, 57000 Kuala Lumpur, MALAYSIA
5. Engenering Research Centre, MARDI, Headquater Serdang, 43400 Serdang, Selangor, MALAYSIA

*ongkhim@upnm.edu.my

Abstract

Citrate reduction of gold (III) chloride trihydrate ($HAuCl_4$) is commonly used method to synthesise citrate-capped gold nanoparticles (cit-AuNPs). In this study, the sequence of reagents addition was modified ("inverse" method) to synthesise smaller size of cit-AuNPs than the standard Turkevich method ("direct" method). Ultraviolet-visible spectroscopy (UV-vis) and field emission transmission electron microscopy (FETEM) confirmed the formation of cit-AuNPs. The cit-AuNPs synthesized using "inverse" method are smaller in size (14.0 ± 3.03 nm) with uniform spherical shape compared to "direct" method (23.5 ± 7.52 nm).

Smaller particles size of cit-AuNPs provide higher efficiency and sensitivity for detection of methylphosphonic acid (MPA) via colorimetric incorporated with image processing with a linear range from 2.5 to 12.5 mM and a low detection limit of 6.28 mM at shorter detection period (24 to 30 s).

Keywords: Gold nanoparticles, sequence reagent additions, methylphosphonic acid, colorimetric, image processing.

Introduction

Nerve agents (NAs) are organophosphonates that can be characterized into three subcategories: G agents, V agents and Novichok agents.[9] They are considerably toxic[19] which cause paralysis and mortality as neural transmission was blocked by permanently binding of NAs with acetylcholinesterase enzyme.[13] Moreover, they rapidly hydrolyze to alkyl methylphosphonic acids (AMPAs) which further hydrolyze into methylphosphonic acid (MPA).[5]

In addition, the hydrolysis product of NA has been classified as Schedule 2B4 category by the Chemical Weapon Convention (CWC). Thus, MPA is an important marker of NA for the verification of CWC.[13] Therefore, development of highly sensitive, rapid analysis, cost-effective and portable sensors have been developed during the last decade.[16]

**** Author for Correspondence***

In recent years, the use of gold nanoparticles (AuNPs) as sensing probe in colorimetry has been extensively discovered owing to their unique plasmonic and photonic characteristic.[8,11,20] According to Wang and Yu[20] highly functional molecular probes can be generated as the physical properties of AuNPs (i.e. optical, magnetic and electronic properties) can be improved by controlling their sizes, shapes, compositions and surface chemistry.

Citrate reduction is the most prevalent conventional method used to synthesize AuNPs. It was developed by Turkevich et al[15] in 1951 by employing only three starting materials namely sodium citrate (Na-cit), hydrochloroauric acid ($HAuCl_4$) and water. In previous reports, synthesized AuNPs were capped with lipoic acid[14], ammonium group[7], citrate[4] and cysteine[2] and applied to detect NAs (GB, GD and VX), mercuric ion, aluminium ion and organophosphate, respectively.

Additionally, the quality and size of the synthesized AuNPs could be affected by altering the order of reagents addition as reported by Ojea-Jiménez et al.[12] Therefore, the effect of different particle sizes of cit-AuNPs on detection of MPA was investigated in this study by two different sequences of reagents addition (Na-cit and $HAuCl_4$).

These two distinct strategies were performed by (i) a "direct" method (Na-cit solution was added into a boiling $HAuCl_4$ solution) and (ii) an "inverse" method ($HAuCl_4$ solution was dropwise into a boiling Na-Cit solution). Subsequently, the synthesised AuNPs by both methods were employed to detect MPA.

Material and Methods

Materials: Gold (III) chloride trihydrate ($HAuCl_4.3H_2O$) was purchased from Sigma (USA). Tri-sodium citrate dihydrate ($C_6H_5Na_3O_7.2H_2O$) and methylphosphonic acid ($CH_3P(O)(OH)_2$) were purchased from Merck (Germany). All chemicals were of analytical grade which were directly used without any purification. Ultrapure water (resistivity of 18.2 MΩ.cm,) was obtained from a Milli-Q water purification system (Millipore) and used for preparing and dilutions of all solutions.

Preparation of citrate-capped gold nanoparticles

"Direct" synthesis of citrate-capped gold nanoparticles: Cit-AuNPs were synthesized according to the chemical reduction method reported by Turkevich et al.[15] Briefly, 100 mL of 0.25 mM of $HAuCl_4$ was boiled to 100°C in 250 mL conical flask at 1500 rpm stirring speed. After 15 min, Na-cit solution (2 mL, 34 mM) was added into the boiling $HAuCl_4$ solution which resulted in a change of solution color from pale yellow to wine red. Subsequently, the mixture was boiled for another 20 min at constant stirring speed and then the solution was allowed to cool to room temperature and kept at 4°C.

"Inverse" citrate-capped gold nanoparticles synthesis: The synthesis of cit-AuNPs was repeated with different sequences of reagent addition based on modification of the method reported by Ojea-Jiménez et al.[12] A colorless solution of Na-cit (100 mL, 0.34 mM) was first boiled for 15 min prior to the addition of $HAuCl_4$ (0.5 mL, 25 mM). Then, the mixture was continuously stirred at 1500 rpm for 20 min at 100°C before cooling down to room temperature and stored at 4°C.

Characterization of "direct" and "inverse" synthesized citrate capped-gold nanoparticles

Fourier transform infrared spectroscopy: Functional groups of synthesized cit-AuNPs were analyzed using universal attenuated total reflectance Fourier transform infrared spectrophotometer (UATR-FTIR) (IRTracer-100, Shimadzu, Japan). A drop of synthesized cit-AuNPs was drop-casted on a top of diamond crystal plate. The spectral resolution was 4 cm^{-1} and scanned in a range of 400 to 4000 cm^{-1}.

Ultraviolet-visible spectrometry analysis: Formation of cit-AuNPs was evaluated by ultraviolet-visible spectrophotometer (UV-vis) (Genesys 6, Thermo Scientific) which operated at a resolution of 1 nm. The absorbance spectrum was scanned from 200 to 800 nm after baseline correction at room temperature using ultrapure water as a reference.

Field emission transmission electron microscopy analysis: Morphology of cit-AuNPs was observed by field emission transmission electron microscope (FETEM) (JEM-2100F, JEOL) which was operated at 200 kV.

A sample of 10 uL of cit-AuNPs was drop-casted onto the carbon-coated copper grid (400-mesh) and allowed to dry in the air in order to evaluate the particles size and their distributions. Subsequently, 50 cit-AuNPs particles were measured by ImageJ software to obtain the particles size.

Preparation of stock solution of methylphosphonic acid: An amount of 2.5 g of MPA was dissolved in Milli-Q ultrapure water to prepare a stock solution (100 mM) and stored at room temperature. Different concentrations of 5 mM, 10 mM, 15 mM, 20 mM and 25 mM of MPA were freshly prepared using Milli-Q ultrapure water by dilution series.

Methylphosphonic acid detection: The synthesized cit-AuNPs were used as chemical sensor for MPA detection where 500 mL of MPA (5 to 25 mM) were added to 500 mL of cit-AuNPs. Detection period and color changed were recorded after shaking gently. All the experimental runs were conducted in triplicate using both cit-AuNPs synthesized from "direct" and "inverse" methods.

Color image processing: After each MPA detection, a color image was captured using a 20-Mega Pixel smart phone (Huawei P20) at a distance of 9 cm in an image capturing box. All conditions including distance, placement of sample in the image capturing box and camera setting were kept constant for all experiments. Digital values of red (R) of the color images were obtained using ImageJ software and employed for further statistical analysis.

Statistical data analysis: In order to determine the significant color change after the detection of MPA, independent *t*-test was analysed using Minitab software version 18.0 (Minitab Inc., PA, USA). The limit of detection (LOD) was calculated based on the equation as reported by Bala et al.[3]

Results and Discussion

Alteration of the Sequence of Reagents Addition: Fig. 1 shows wide-scan FTIR spectra (4000 - 400 cm^{-1}) of both cit-AuNPs from "direct" and "inverse" synthesis methods. The broad absorbance peak of O-H stretching vibration at 3300 cm^{-1} in both spectra is due to the presence of water in both cit-AuNPs solutions. An absorption peak located at 1631 cm^{-1} is indicative of the carboxylate (COO^-) asymmetric stretching band from the COOH group of citrate in both cit-AuNPs. A similar carboxylate asymmetric stretching band (1591 cm^{-1}) of cit-AuNPs was reported by Wulandari et al.[21]

Fig. 2 shows a comparison of the UV-vis absorption spectroscopy of the cit-AuNPs synthesized by both "direct" and "inverse" methods. Fig. 2a inset and 2b inset show visual evidences of cit-AuNPs synthesized from "inverse" and "direct" synthesis methods respectively. The results revealed that "inverse" synthesis method produced a lighter red color of cit-AuNPs solution than "direct" synthesis method.

This is due to the color of cit-AuNPs solutions obtained varying according to their size.[17] The maximum absorption peaks for "direct" and "inverse" synthesis methods were found at 522 nm and 519 nm respectively. Both cit-AuNPs displayed absorption peaks in the visible range. Remarkably, there was a red shifting of surface plasmon resonance (SPR) peak from 519 nm ("inverse" synthesis method) to 522 nm ("direct" synthesis method) together with an increase of the absorbance maximum value which may be attributed to the surface plasmon oscillation of free electrons accordance to Mie theory.[6]

Fig. 3 displays the FETEM images of cit-AuNPs with different synthesis methods via "direct" and "inverse". ImageJ was used to determine the size of cit-AuNPs by measuring the diameter of particles on FETEM images. Both FETEM images and particles size distribution histograms (Fig. 4) clearly confirmed a decrease of the mean particles size (14.0 ± 3.03 nm) of cit-AuNPs obtained from "inverse" synthesis method compared to that of (23.5 ± 7.52 nm) "direct" synthesis method. Moreover, the FETEM images show that most of the cit-AuNPs produced from both synthesis methods were round and spherical in shape. As reported by Verma et al[17], a spherical shape of cit-AuNPs is due to negative charged layer of citrate ions repelling each other.

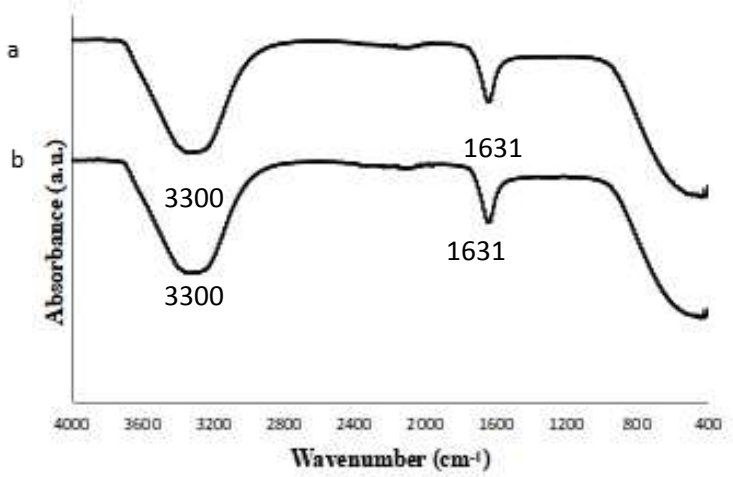

Fig. 1: FTIR spectra of cit-AuNPs synthesized via (a) "direct" and (b) "inverse" methods.

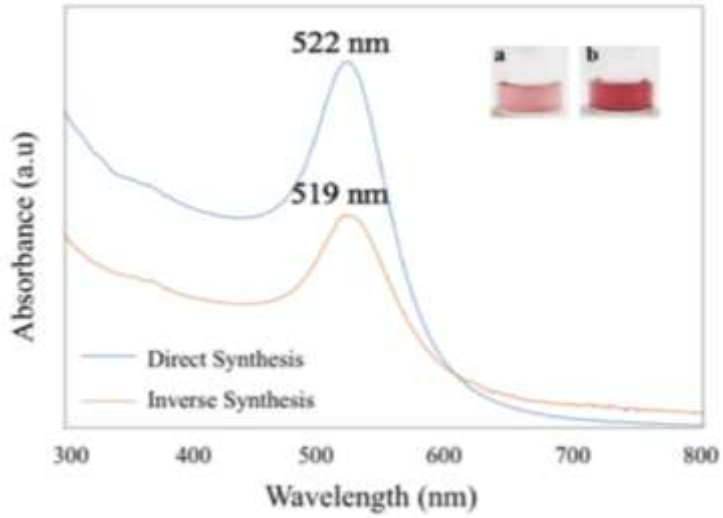

Fig. 2: UV-vis spectra of cit-AuNPs synthesized via a) inverse (519 nm) and b) direct (522 nm) methods.

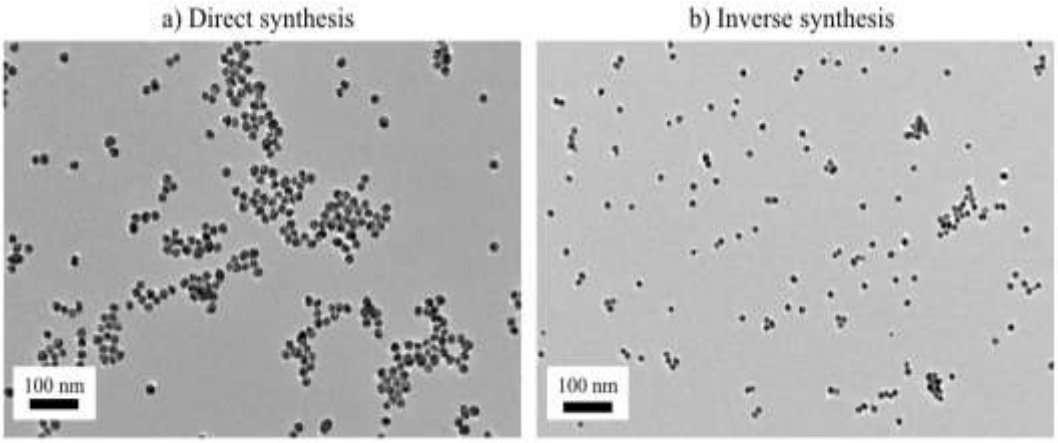

Fig. 3: FETEM micrographs of cit-AuNPs synthesized via (a) direct and (b) inverse methods.

Detection on Methylphosphonic Acid (MPA) by colorimetry incorporated with image processing: The colorimetric method was employed for detection of MPA where different concentrations of MPA were spiked into both cit-AuNPs "direct" and "inverse" synthesis methods, respectively. As shown in fig. 5 and fig. 6, SPR absorption bands got shifted from 522 nm to 680 nm and from 519 nm to 710 nm using cit-AuNPs synthesized from "direct" and "inverse" methods respectively, after the addition of MPA. Marti et al[10] explained that shifting of SPR absorption band is due to aggregation of nanoparticles triggered by the change in the overall electrostatic charge on the surfaces of nanoparticles. The aggregation of cit-AuNPs in this study was further confirmed by FETEM analysis (Fig. 7).

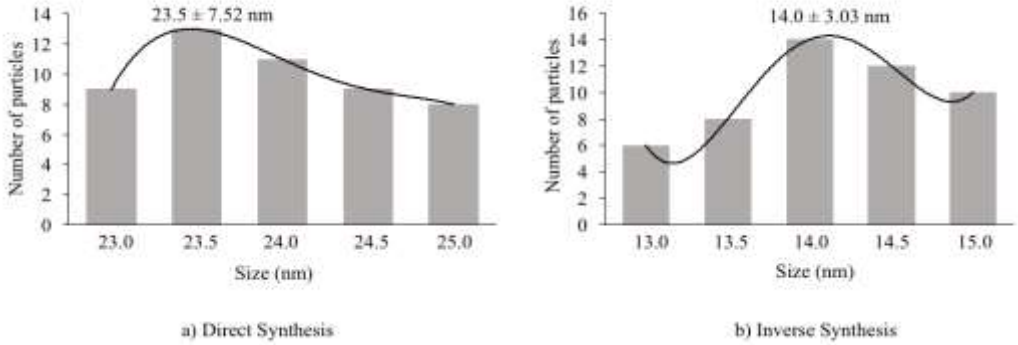

Fig. 4: Particles size distribution of AuNPs synthesized by (a) direct and (b) inverse methods.

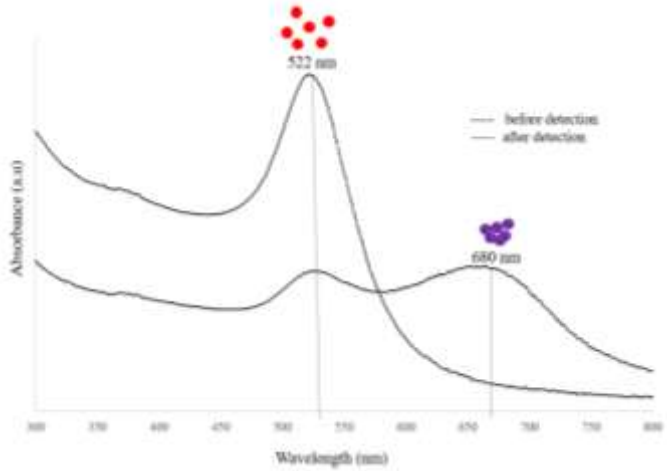

Fig. 5: UV- vis spectra of cit-AuNPs before and after detection of 12.5 mM of MPA using cit-AuNPs synthesized by direct method.

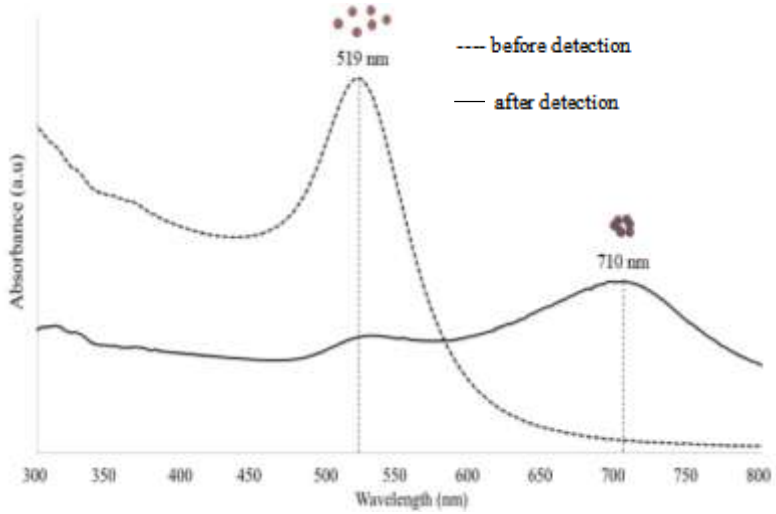

Fig. 6: UV- vis spectra of cit-AuNPs before and after detection of 12.5 mM of MPA using cit-AuNPs synthesized by inverse method.

ImageJ was used to measure the color intensities [red (R), green (G) and blue (B) values] of AuNPs-MPA complex formed. The background color was removed in the images color threshold, converted to grey scale and the RGB values were determined. Based on the digital values of RGB (Tables 2 and 3), the intensities of R decreased with increasing of MPA concentration.

The maximum absorption of UV-vis at 680 nm and 710 nm (which matches the red light region) was observed after detection of MPA using cit-AuNPs "direct" and "inverse" synthesis methods respectively (Figures 5 and 6). Therefore, ΔR value was used for MPA determination where ΔR was calculated based on the differences between the R value of blank and the R value of the complex formed.

As shown in tables 2 and 3, cit-AuNPs from "inverse" synthesis method offered larger ΔR value and a shorter detection period compared to that of "direct" synthesis method. This is due to smaller particles size of cit-AuNPs being produced in "inverse" synthesis method which is more colloidally stable[18] and has s larger surface-to-volume ratios[20] and readily reacts with MPA.

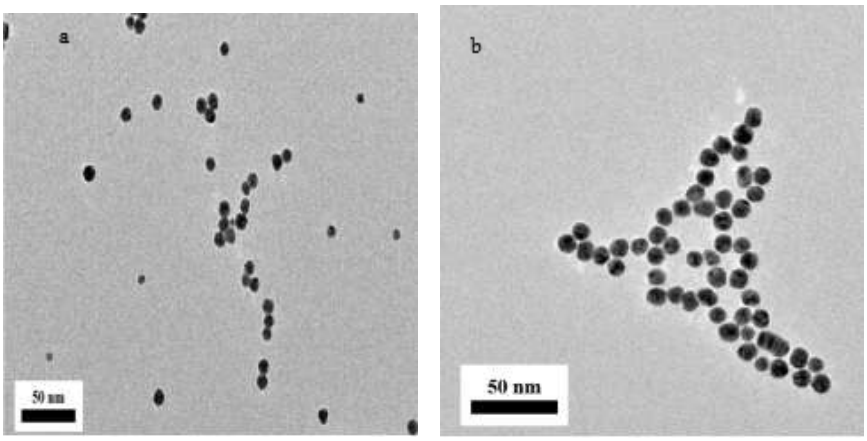

Fig. 7: FETEM micrographs of cit-AuNPs-MPA (a) before detection and (b) after detection of MPA using inverse cit-AuNPs method.

Table 2
The ΔR value of cit-AuNPs-MPA formed using cit-AuNPs synthesized by "direct" method to detect different concentrations of MPA (2.5 – 12.5 mM).

Final concentration of MPA (mM)	Mean value of R ± SD	Mean value of ΔR
0	133.68 ± 0.98	-
2.5	130.84 ± 0.09	2.84
5.0	127.37 ± 0.19	6.31
7.5	118.79 ± 0.38^{A}	14.89
10.0	114.26 ± 0.35^{A}	19.42
12.5	101.21 ± 0.11^{A}	32.47

Significant differences among R values of blank and samples after detection of MPA by "direct" synthesis method of cit-AuNPs:
^{A} $P \leq 0.05$

Table 3
The ΔR value of cit-AuNPs-MPA formed using cit-AuNPs synthesized by "inverse" method to detect different concentrations of MPA (2.5 – 12.5 mM).

Final concentration of MPA (mM)	Mean value of R ± SD	Mean value of ΔR
0	157.34 ± 0.23	-
2.5	146.05 ± 0.31^{B}	11.29
5.0	137.72 ± 0.39^{B}	19.62
7.5	128.60 ± 0.71^{B}	28.74
10.0	115.31 ± 0.60^{B}	42.03
12.5	111.54 ± 0.39^{B}	45.80

Significant differences among R values of blank and samples after detection of MPA by "inverse" synthesis method of cit-AuNPs:
^{B} $P \leq 0.05$

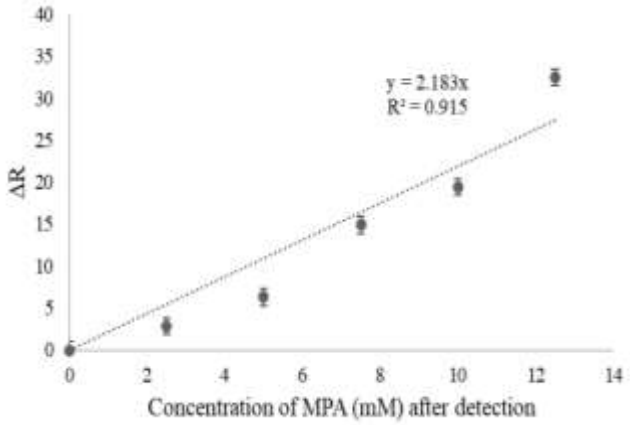

Fig. 8: Calibration curve of cit-AuNPs synthesized using the "direct" method. Error bars indicate the standard deviation (SD) of ΔR with n=3.

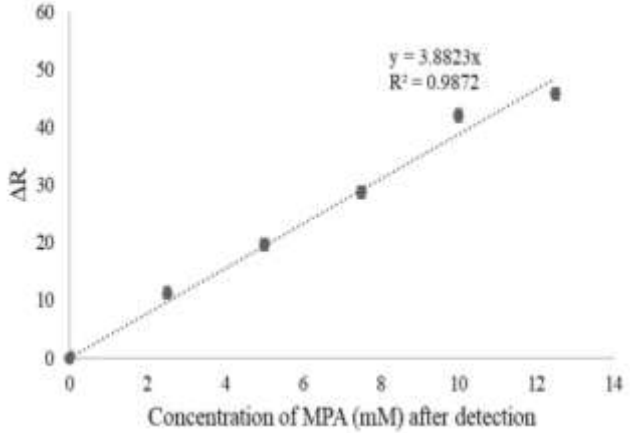

Fig. 9: Calibration curve of cit-AuNPs synthesized using the "inverse" method. Error bars indicate the standard deviation (SD) of ΔR with n=3.

Limit of detection (LOD) is an important parameter to evaluate the performance of a sensor. Figures 8 and 9 show the calibration curves for detection of MPA using cit-AuNPs synthesized from "direct" and "inverse" synthesis method respectively. Cit-AuNPs from "inverse" synthesis method showed a linear response with higher linear regression of 0.9872 over difference concentrations of MPA as compared to the "direct" synthesis cit-AuNPs method with only 0.915. The calculated LOD were 6.28 mM and 13.68 mM for "inverse" and "direct" synthesis method respectively. Thus, cit-AuNPs synthesized from "inverse" synthesis method was more sensitive in detection of MPA.

Conclusion

Different particle sizes of cit-AuNPs have been produced using the "inverse" and "direct" methods. The cit-AuNPs synthesized by "inverse" method are smaller in size (14.0 ± 3.03 nm) with an even distribution compared to the "direct" cit-AuNPs method (23.5 ± 7.52 nm). This smaller size of cit-AuNPs provided better performance in MPA detection with LOD of 6.28 mM compared to a bigger size of cit-AuNPs (LOD of 13.68 mM).

Hence, it is suggested that the cit-AuNPs synthesized using "inverse" method are more sensitive for detection of MPA in colorimetric sensors compared to the "direct" synthesis method.

Acknowledgement

This work was supported by Fundamental Research Grant Scheme (FRGS/1/2017/STG01/UPNM/02/1) funded by the Ministry of Higher Education, Malaysia. The authors also would like to thank to Universiti Pertahanan Nasional Malaysia for providing the laboratory facilities.

References

1. Patel R.M., Patel D.M., Shah K.P. and Patel D.A., Synthesis of Polyketones and their Antimicrobial Study, *Res. J. Chem. Environ.*, **3(2)**, 47 **(1999)**

2. Bala R., Sharma R.K. and Wangoo N., Highly Sensitive Colorimetric Detection of Ethyl Parathion using Gold Nanoprobes, *Sensors and Actuators B: Chemical.*, **210**, 425-430 **(2015)**

3. Bala R., Kumar M., Bansal K., Sharma R.K. and Wangoo N., Ultrasensitive aptamer biosensor for malathion detection based on cationic polymer and gold nanoparticles, *Biosensors and Bioelectronics*, **15(85)**, b 445-449 **(2016)**

4. Chen S., Fang Y.M., Xiao Q., Li J., Li S.B., Chen H.J. and Yang H.H., Rapid Visual Detection of Aluminium Ion using Citrate Capped Gold Nanoparticles, *Analyst*, **137(9)**, 2021-2023 **(2012)**

5. Katagi M., Nishikawa M., Tatsuno M. and Tsuchihashi H., Determination of The Main Hydrolysis Products of Organophosphorus Nerve Agents, Methylphosphonic Acids, in Human Serum by Indirect Photometric Detection Ion Chromatography, *Journal of Chromatography B: Biomedical Sciences and Applications*, **698(1-2)**, 81-88 **(1997)**

6. Liang A., Liu Q., Wen G. and Jiang Z., The Surface-Plasmon-Resonance Effect of Nanogold/Silver and its Analytical Applications, *TrAC Trends in Analytical Chemistry*, **37**, 32-47 **(2012)**

7. Liu D., Qu W., Chen W., Zhang W., Wang Z. and Jiang X., Highly Sensitive, Colorimetric Detection of Mercury (II) in Aqueous Media by Quaternary Ammonium Group-Capped Gold Nanoparticles at Room Temperature, *Analytical Chemistry*, **82(23)**, 9606-9610 **(2010)**

8. Ma J. and Li C.W., Rapid and Continuous Parametric Screening for The Synthesis of Gold Nanocrystals with Different Morphologies using a Microfluidic Device, *Sensors and Actuators B: Chemical.*, **262**, 236-244 **(2018)**

9. Makinen M.A., Anttalainen O.A. and Sillanpää M.E., Ion Mobility Spectrometry and Its Applications In Detection of Chemical Warfare Agents, *Analytical Chemistry*, **82(23)**, 9594-9600 **(2010)**

10. Martí A., Costero A.M., Gaviña P., Gil S., Parra M., Brotons-Gisbert M. and Sánchez-Royo J.F., Functionalized Gold Nanoparticles as an Approach to the Direct Colorimetric Detection of DCNP Nerve Agent Simulant, *European Journal of Organic Chemistry*, **2013(22)**, 4770-4779 **(2013)**

11. Nair K.K., Srivastava N., Kumari S., Alam S. and Raza S.K., Significance of Nanotechnology for Sensing, Estimation, Degradation and Formulation of Agrochemicals, Impact of Nanoscience in the Food Industry, 217-276 **(2018)**

12. Ojea-Jiménez I., Bastús N.G. and Puntes V., Influence of the Sequence of the Reagents Addition in the Citrate-Mediated Synthesis of Gold Nanoparticles, *The Journal of Physical Chemistry C.*, **115(32)**, 15752-15757 **(2011)**

13. Sathe M., Ghorpade R., Merwyn S., Agarwal G.S. and Kaushik M.P., Direct Hapten-Linked Competitive Inhibition Enzyme-Linked Immunosorbent Assay (CIELISA) for the Detection of O-pinacolyl Methylphosphonic acid, *Analyst*, **137(2)**, 406-413 **(2012)**

14. Sun J., Guo L., Bao Y. and Xie J., A Simple, Label-free AuNPs-based Colorimetric Ultrasensitive Detection of Nerve Agents and Highly Toxic Organophosphate Pesticide, *Biosensors and Bioelectronics*, **28(1)**, 152-157 **(2011)**

15. Turkevich J., Stevenson P.C. and Hillier J., A Study of the Nucleation and Growth Processes in the Synthesis of Colloidal Gold, *Discussions of the Faraday Society*, **11**, 55-75 **(1951)**

16. Upadhyayula V.K.K., Functionalized Gold Nanoparticle Supported Sensory Mechanisms Applied in Detection of Chemical and Biological Threat Agents: A Review, *Analytica Chimica Acta*, **715**, 1-18 **(2012)**

17. Verma H.N., Singh P. and Chavan R.M., Gold Nanoparticle: Synthesis and Characterization, *Veterinary World*, **7(2)**, 72 **(2014)**

18. Verma M.S., Rogowski J.L., Jones L. and Gu F.X., Colorimetric Biosensing of Pathogens Using Gold Nanoparticles, *Biotechnology Advances*, **33(6)**, 666-680 **(2015)**

19. Vernekar A.A., Das T. and Mugesh G., Vacancy-Engineered Nanoceria: Enzyme Mimetic Hotspots for the Degradation of Nerve Agents, *Angewandte Chemie International Edition*, **55(4)**, 1412-1416 **(2016)**

20. Wang C. and Yu C., Detection of Chemical Pollutants in Water using Gold Nanoparticles as Sensors: A Review, *Reviews in Analytical Chemistry*, **32(1)**, 1-14 **(2013)**

21. Wulandari P., Nagahiro T., Fukada N., Kimura Y., Niwano M. and Tamada K., Characterization of Citrates on Gold and Silver Nanoparticles, *Journal of Colloid and Interface Science*, **438**, 244-248 **(2015)**.

(Received 08th April 2020, accepted 08th June 2020)